
Supplementary material: Ensembling geophysical models with Bayesian Neural Networks

Anonymous Author(s)
Affiliation
Address
email

1 Contents

2	A Construction of ozone baselines	1
3	A.1 Multi-model mean	1
4	A.2 Weighted mean	2
5	A.3 Spatially weighted mean	2
6	A.4 Spatiotemporal kriging	2
7	A.5 Bilinear interpolation	2
8	B Hyperparameter details	2
9	C Derivation of loss function	3
10	D Extra ozone experiment plots	4
11	D.1 Bias	4
12	D.2 Epistemic uncertainty	4
13	D.3 Average model weight	4

14 A Construction of ozone baselines

15 We remind the reader that all of these baselines use the same data for training, testing and validation
16 as the Bayesian neural network ensemble. This validation tests the ability of the ensembling methods
17 to interpolate and extrapolate, particularly over regions of interest and sparse data.

18 A.1 Multi-model mean

19 This is the uniform weighting of all the 15 chemistry-climate models. The prediction is therefore,

$$y_{\text{MMM}}(\mathbf{x}, t) = \frac{1}{15} \sum_{i=1}^{15} M_i(\mathbf{x}, t) \quad (1)$$

20 where $y_{\text{MMM}}(\mathbf{x}, t)$ is the multi-model mean prediction and $M_i(\mathbf{x}, t)$ is the i -th individual model
21 prediction.

22 A.2 Weighted mean

23 Here the ensemble mean is constructed from model projections weighted by their skill (in replicating
24 observations) and their independence. This is based on work from Knutti et al. [2], Sanderson et al.
25 [3]. For an ensemble of N models, the weight for model i (w_i) is given by

$$w_i = \exp\left(-\frac{D_i^2}{n_i\sigma_D^2}\right) / \left(1 + \sum_{j \neq i}^N \exp\left(-\frac{S_{ij}^2}{n_i\sigma_S^2}\right)\right), \quad (2)$$

26 where D_i^2 is the squared difference between a model and observation averaged over all space and
27 time, S_{ij}^2 is the squared difference between models averaged over all space and time, n_i is the size
28 of data used in constructing the weight, and σ_D and σ_S are constants which allow tuning of the
29 weighting. The weights w_i are normalise to sum to 1. The weighted prediction is therefore

$$y_{WM}(\mathbf{x}, t) = \sum_{i=1}^N w_i M_i(\mathbf{x}, t). \quad (3)$$

30 Values of σ_D and σ_S were found by minimising the difference between the weighted prediction and
31 the observations over the training data.

32 A.3 Spatially weighted mean

33 The ensemble is constructed much the same as the weighted mean presented above, except that model
34 weights vary in space. The weights are calculated

$$w_i(\mathbf{x}, t) = \exp\left(-\frac{D_i(\mathbf{x}, t)^2}{n_i(\mathbf{x}, t)\sigma_D^2}\right) / \left(1 + \sum_{j \neq i}^N \exp\left(-\frac{S_{ij}(\mathbf{x}, t)^2}{n_i(\mathbf{x}, t)\sigma_S^2}\right)\right), \quad (4)$$

35 and are used to generate the prediction,

$$y_{SWM}(\mathbf{x}, t) = \sum_{i=1}^N w_i(\mathbf{x}, t) M_i(\mathbf{x}, t). \quad (5)$$

36 A.4 Spatiotemporal kriging

37 We performed spatiotemporal kriging using an implementation of a stochastic variational Gaussian
38 process (SVGP) from GPFlow [1]. Due to the size of the training data (1.8 million data points) we
39 used a SVGP on 3 year sections of observational data with 5000 inducing points per section. The
40 kernel we used was the product of a Matern3/2 kernel acting over latitude and time, and periodic
41 Matern3/2 kernel acting over longitude. We used an Adam optimiser implemented in tensorflow to
42 train the SVGP.

43 A.5 Bilinear interpolation

44 Bilinear interpolation over the training data was performed using the SciPy function grid-
45 data: <https://docs.scipy.org/doc/scipy/reference/generated/scipy.interpolate.griddata.html>.

47 B Hyperparameter details

48 The pretrained model weights and the code to run the BayNNE for both the syn-
49 thetic and ozone experiments can be found here: <https://anonymous.4open.science/r/6bf08e5a-c909-45a3-be63-aa0f5ba187df/>. Table 1 shows the hyperparameters chosen in
50 the running of the BayNNE for both experiments.

51
52 The heteroscedastic loss function is prone to episodes of catastrophic forgetting. To avoid these, we
53 use large batch sizes, small learning rates and a large number of epochs so that each neural network
54 ensemble member may be stably trained till convergence.

Table 1: Hyperparameter values and priors for BayNNE.

	Synthetic experiment	Ozone experiment
Spatial coord scaling	2	2
Temporal coord scaling (month of year)	1	2
Temporal coord scaling (total months)	1	1
Number of physical models	4	15
Number of neural network ensemble members	50	65
Bias mean. prior	0	0
Bias std. prior	0.01	0.03
Noise mean prior	0.02	0.015
Noise std. prior	0.004	0.003
Number of hidden layers	1	1
Number of hidden nodes	100	500
Optimiser	Adam	Adam
Batch Size	2000	25000
Learning rate	5×10^{-5}	3×10^{-5}
Number of epochs	6000	125000

55 The neural network ensemble for the 2 million datapoint ozone dataset were trained across a cluster
 56 of 6 P100 GPUs. Each neural network needed 20 hours to be trained till convergence and the entire
 57 ensemble needed 8 days of wall clock time.

58 C Derivation of loss function

59 In the following, we derive the anchored ensembling loss function for the heteroscedastic case. For
 60 the j -th neural network ensemble member in randomized MAP sampling, we compute the MAP
 61 estimate corresponding to a recentered prior over parameters $\theta_{anc,j}$, $P(\theta_j) = \mathcal{N}(\theta_{anc,j}, \Sigma_{prior})$.
 62 Here $\theta_{anc,j}$ is a sample from the original multivariate normal prior over parameters, i.e. $\theta_{anc,j} \sim$
 63 $\mathcal{N}(\mu_{prior}, \Sigma_{prior})$.

$$\begin{aligned}
 \theta_{MAP,j} &= \operatorname{argmax}_{\theta_j} P(\theta_j | \mathcal{D}) \\
 &= \operatorname{argmax}_{\theta_j} P_{\mathcal{D}}(\mathcal{D} | \theta_j) P(\theta_j) \quad (\text{Bayes' Theorem}) \\
 &= \operatorname{argmax}_{\theta_j} \log(P_{\mathcal{D}}(\mathcal{D} | \theta_j)) + \log(P(\theta_j)) \quad (\text{log strictly monotonic increasing}) \\
 &= \operatorname{argmax}_{\theta_j} \log(P_{\mathcal{D}}(\mathcal{D} | \theta_j)) - \frac{1}{2} (\theta_j - \theta_{anc,j})^T \Sigma_{prior}^{-1} (\theta_j - \theta_{anc,j}) + \text{const.} \\
 &= \operatorname{argmax}_{\theta_j} \log(P_{\mathcal{D}}(\mathcal{D} | \theta_j)) - \frac{1}{2} \|\Sigma_{prior}^{-1/2} (\theta_j - \theta_{anc,j})\|_2^2 \quad (\text{diagonal prior covariance})
 \end{aligned}$$

64 If we specify the data likelihood for our regression task assuming i.i.d. observations and additive
 65 heteroscedastic Gaussian noise i.e., $P_{\mathcal{D}}(\mathcal{D} | \theta_j) = \prod_{i=1}^{N_D} \mathcal{N}(\hat{y}_j(\mathbf{x}_i, t_i), \sigma_j^2(\mathbf{x}_i, t_i))$, we obtain

$$\begin{aligned}
 \theta_{MAP,j} &= \operatorname{argmax}_{\theta_j} - \frac{1}{2} \sum_{i=1}^{N_D} \frac{(y_i - \hat{y}_j(\mathbf{x}_i, t_i))^2}{\sigma_j^2(\mathbf{x}_i, t_i)} - \sum_{i=1}^{N_D} \log(\sigma_j(\mathbf{x}_i, t_i)) + \text{const.} - \frac{1}{2} \|\Sigma_{prior}^{-1/2} (\theta_j - \theta_{anc,j})\|_2^2 \\
 &= \operatorname{argmin}_{\theta_j} \sum_{i=1}^{N_D} \frac{(y_i - \hat{y}_j(\mathbf{x}_i, t_i))^2}{\sigma_j^2(\mathbf{x}_i, t_i)} + \sum_{i=1}^{N_D} \log(\sigma_j^2(\mathbf{x}_i, t_i)) + \|\Sigma_{prior}^{-1/2} (\theta_j - \theta_{anc,j})\|_2^2 \quad (\times -2 \text{ throughout})
 \end{aligned}$$

66 **D Extra ozone experiment plots**

67 In the main text we highlighted the models with the most interesting features and highest weights.
68 For completeness here, we include a wider range of plots looking at model weights and modelled
69 bias and uncertainties, for the ozone experiment.

70 **D.1 Bias**

71 Figures 1 and 2 show the modelled bias averaged in time and space respectively. Bias is seen to be
negative over polar regions especially the southern polar region and southern mid latitudes.

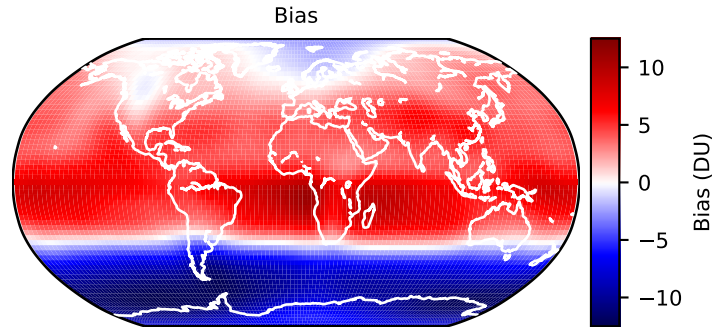


Figure 1: Temporally averaged modelled bias.

72

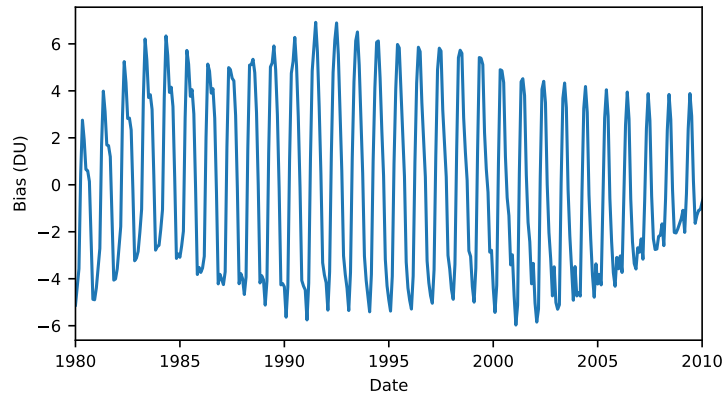


Figure 2: Spatially averaged modelled bias.

73 **D.2 Epistemic uncertainty**

74 Figures 3 and 4 show the epistemic uncertainty averaged in time and space respectively. Epistemic
75 uncertainty is highest at polar regions. Epistemic uncertainty increases for regions with sparse or no
76 data including 2007–2010 (used to validate extrapolation) and 1993–1997 where there is a greater
77 sparsity of data. This can be seen clearly in Figure 4.

78 **D.3 Average model weight**

79 Figure 5 shows the average model weight for all 15 chemistry-climate models used in the ozone
80 experiment.

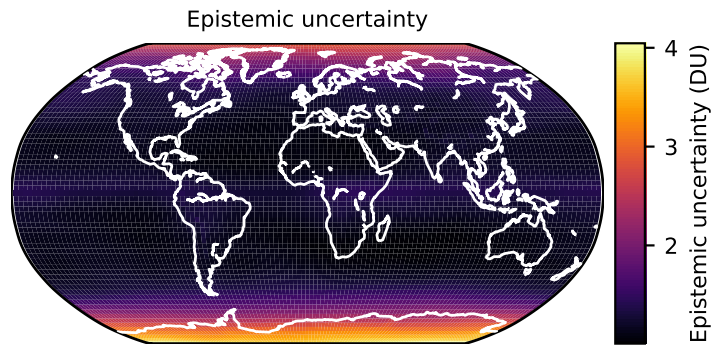


Figure 3: Temporally averaged epistemic uncertainty.

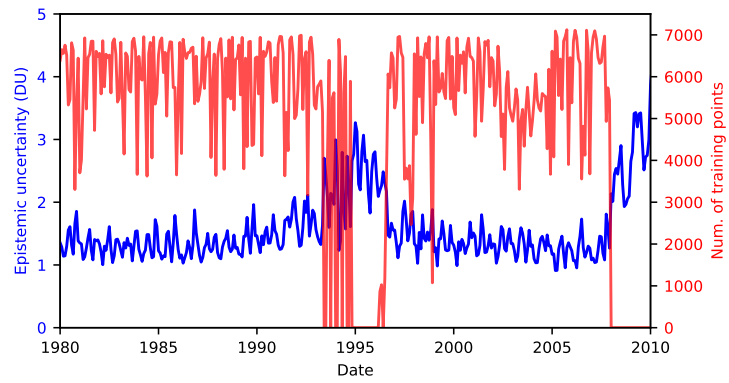


Figure 4: Spatially averaged epistemic uncertainty and the number of training points per month.

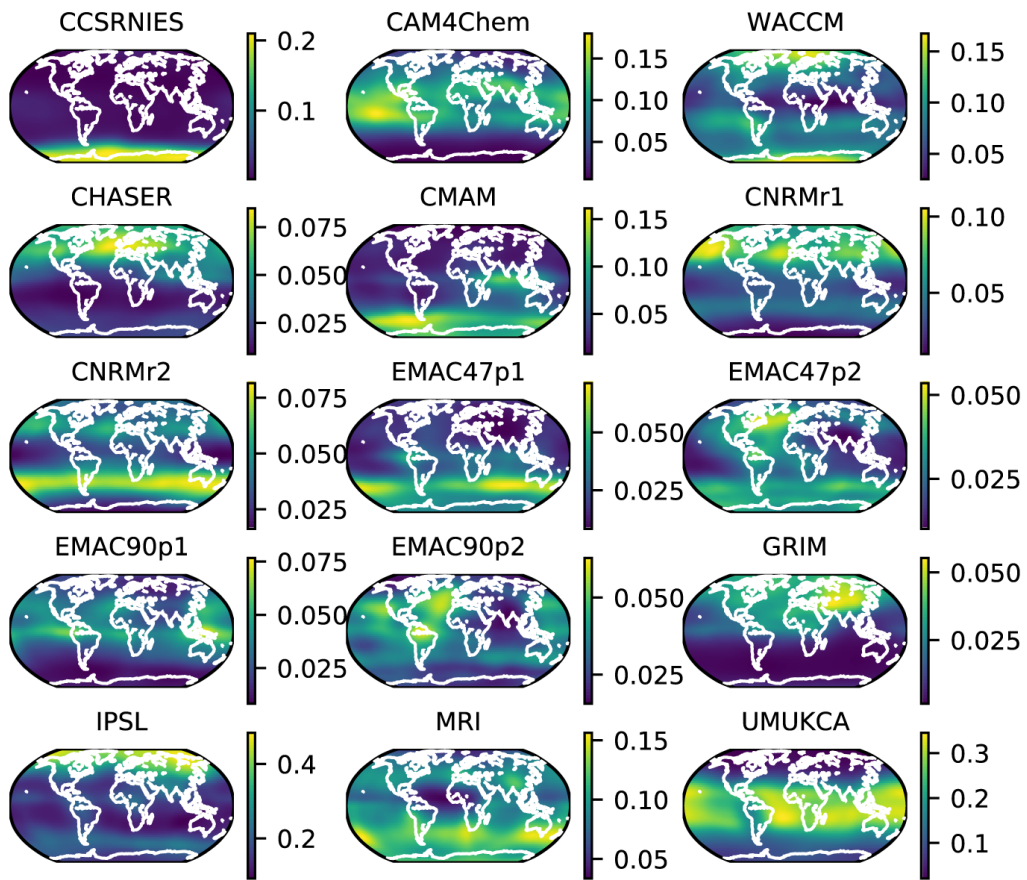


Figure 5: Temporally averaged model weights for all 15 chemistry-climate models.

81 **References**

- 82 [1] A. G. De G. Matthews, M. Van Der Wilk, T. Nickson, K. Fujii, A. Boukouvalas, P. León-Villagrà,
83 Z. Ghahramani, and J. Hensman. Gpflow: A gaussian process library using tensorflow. *J. Mach.*
84 *Learn. Res.*, 18(1):1299–1304, Jan. 2017. ISSN 1532-4435.
- 85 [2] R. Knutti, J. Sedláček, B. M. Sanderson, R. Lorenz, E. M. Fischer, and V. Eyring. A climate model
86 projection weighting scheme accounting for performance and interdependence. *Geophysical*
87 *Research Letters*, 44(4):1909–1918, 2017. doi: 10.1002/2016GL072012.
- 88 [3] B. M. Sanderson, M. Wehner, and R. Knutti. Skill and independence weighting for multi-
89 model assessments. *Geoscientific Model Development*, 10(6):2379–2395, 2017. doi: 10.5194/
90 gmd-10-2379-2017.